

1 **Ceftazidime Is a Potential Drug to Inhibit SARS-CoV-2 Infection In Vitro by Blocking**
2 **Spike Protein-ACE2 Interaction**

3 ChangDong Lin^{1,4}, Yue Li^{1,4}, MengYa Yuan¹, MengWen Huang¹, Cui Liu¹, Hui Du¹,
4 XingChao Pan¹, YaTing Wen¹, Xinyi Xu², Chenqi Xu^{2,3} and JianFeng Chen^{1,3,*}

5 ¹State Key Laboratory of Cell Biology, Shanghai Institute of Biochemistry and Cell
6 Biology, Center for Excellence in Molecular Cell Science, Chinese Academy of Sciences,
7 University of Chinese Academy of Sciences, Shanghai 200031, China

8 ²State Key Laboratory of Molecular Biology, Shanghai Institute of Biochemistry and Cell
9 Biology, Center for Excellence in Molecular Cell Science, Chinese Academy of Sciences,
10 University of Chinese Academy of Sciences, Shanghai 200031, China

11 ³School of Life Science, Hangzhou Institute for Advanced Study, University of Chinese
12 Academy of Sciences, Hangzhou 310024, China.

13 ⁴These authors contributed equally

14 *Correspondence: jfchen@sibcb.ac.cn

15 **SUMMARY**

16 Coronavirus Disease 2019 (COVID-19) spreads globally as a severe pandemic, which is
17 caused by severe acute respiratory syndrome coronavirus 2 (SARS-CoV-2). Cell entry of
18 SARS-CoV-2 mainly depends on binding of the viral spike (S) proteins to angiotensin
19 converting enzyme 2 (ACE2) on host cells. Therefore, repurposing of known drugs to
20 inhibit S protein-ACE2 interaction could be a quick way to develop effective therapy for
21 COVID-19. Using a high-throughput screening system to investigate the interaction
22 between spike receptor binding domain (S-RBD) and ACE2 extracellular domain, we
23 screened 3581 FDA-approved drugs and natural small molecules and identified
24 ceftazidime as a potent compound to inhibit S-RBD-ACE2 interaction by binding to S-
25 RBD. In addition to significantly inhibit S-RBD binding to HPAEpiC cells, ceftazidime
26 efficiently prevented SARS-CoV-2 pseudovirus to infect ACE2-expressing 293T cells.
27 The inhibitory concentration (IC_{50}) was 113.2 μ M, which is far below the blood
28 concentration (over 300 μ M) of ceftazidime in patients when clinically treated with
29 recommended dose. Notably, ceftazidime is a drug clinically used for the treatment of
30 pneumonia with minimal side effects compared with other antiviral drugs. Thus,
31 ceftazidime has both anti-bacterial and anti-SARS-CoV-2 effects, which should be the
32 first-line antibiotics used for the clinical treatment of COVID-19.

33

34 **KEYWORDS**

35 Ceftazidime, SARS-CoV-2, S-RBD, ACE2, COVID-19

36

37 INTRODUCTION

38 Coronavirus disease 2019 (COVID-19) has spread globally as a severe pandemic, which
39 was caused by a novel coronavirus named Severe Acute Respiratory Syndrome coronavirus
40 2 (SARS-CoV-2) ¹. According to the latest statistics of COVID-19 released by Johns
41 Hopkins University on September 1, 2020, there were 25.50 million confirmed cases and
42 0.85 million deaths globally. COVID-19 has become a serious threat to human survival and
43 is likely to coexist with human beings for a long time. Unfortunately, there is still no
44 effective cure for COVID-19, especially the critically ill patients.

45 Similar to SARS-CoV, SARS-CoV-2 belongs to the sarbecoviruses (Betacoronirus,
46 Coronaviridae) and can cause life-threatening respiratory diseases ²⁻⁴. Some mechanisms
47 underlying SARS-CoV-2 infection of target cells have been reported ⁵⁻⁷. Spike (S) protein
48 on the surface of SARS-CoV-2 facilitates viral entry into target cells by mediating virus
49 receptor recognition and membrane fusion. The N-terminal region of its S1 domain
50 contains receptor binding domain (RBD), which directly binds to angiotensin converting
51 enzyme 2 (ACE2) receptor on the plasma membrane of host cells and is responsible for
52 virus attachment ^{8,9}. Therefore, blocking the binding of spike protein to ACE2 is an
53 effective way to inhibit the infection of target cells by SARS-CoV-2. By now, several
54 studies have reported the development of monoclonal antibodies targeting spike protein
55 ^{10,11}, however, the typical timeline for approval of a novel antibody for the management
56 viral infection is long. In addition, the side effects such as antibody-dependent
57 enhancement of viral infection need to be considered ¹¹⁻¹³, and the high cost of antibody
58 treatment will limit the clinical application. Therefore, repurposing of known small

59 molecule drugs to inhibit spike protein and ACE2 binding could significantly accelerate
60 the deployment of effective and affordable therapies for COVID-19.

61 In this study, we expressed and purified Spike-RBD (S-RBD) and the extracellular
62 domain of ACE2 (ACE2-ECD) and then established an AlphaScreen-based high-
63 throughput system for screening small molecules that block S-RBD–ACE2-ECD
64 interaction. From 3581 Food and Drug Administration (FDA)-approved drugs and natural
65 small molecule compounds, we identified 10 compounds that could block S-RBD–ACE2-
66 ECD interaction in the initial screening. Notably, ceftazidime bound to S-RBD and showed
67 the strongest potency for the inhibition of S-RBD binding to human pulmonary alveolar
68 epithelial cells (HPAEpiC). Moreover, ceftazidime efficiently inhibited the infection of
69 ACE2-expressing 293T cells by SARS-CoV-2 pseudovirus. Overall, we identified
70 ceftazidime as a potential drug to inhibit SARS-CoV-2 infection with minimal known side
71 effects and affordable price.

72

73 **RESULTS**

74 **Establishment of AlphaScreen system to detect S-RBD–ACE2 interaction**

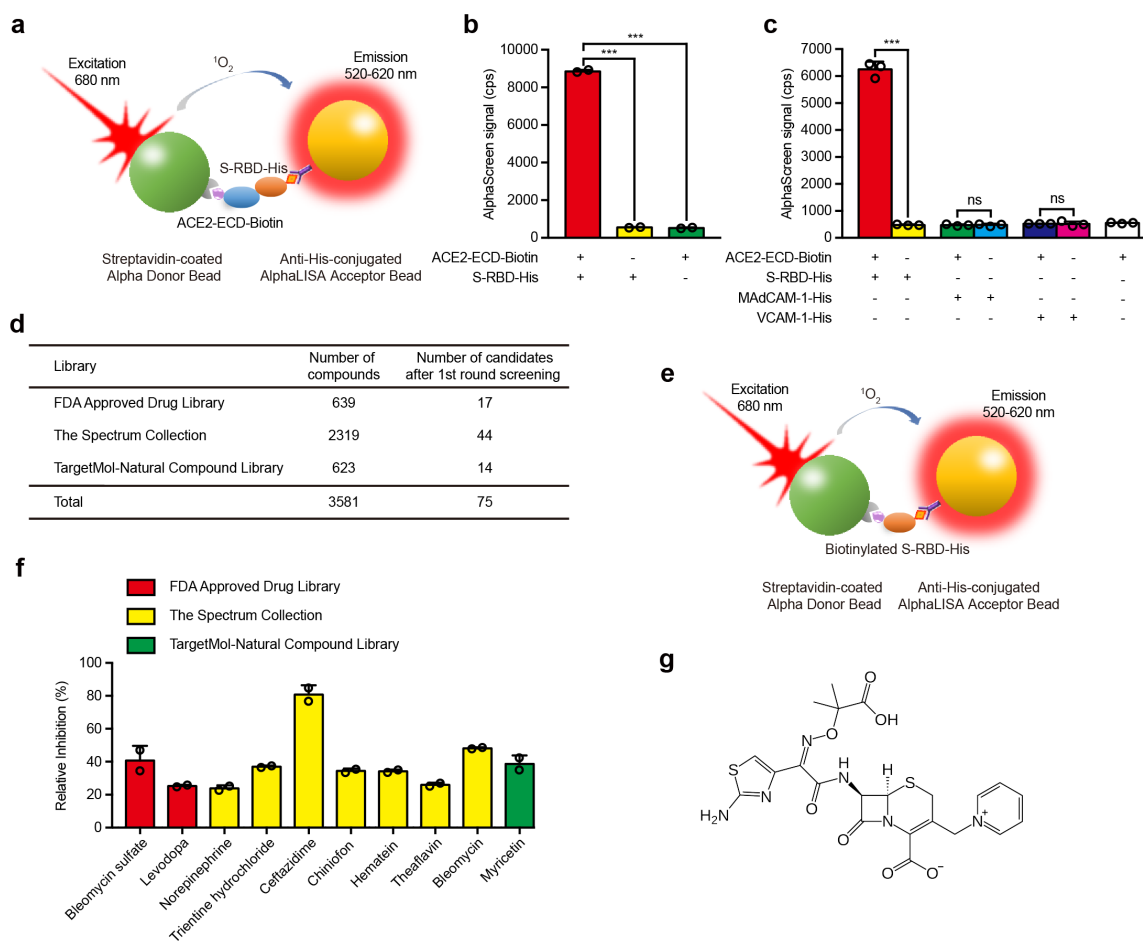
75 In order to screen small molecules that block S protein-ACE2 binding, we firstly
76 established an AlphaScreen-based high-throughput system to detect the interaction
77 between S-RBD and ACE2-ECD (Fig. 1a). S-RBD and ACE2-ECD were expressed in
78 293T cells and then purified. Biotinylated ACE2-ECD (ACE2-ECD-Biotin) binds to
79 streptavidin-coated Alpha donor beads and His-tagged S-RBD (S-RBD-His) binds to anti-
80 His-conjugated AlphaLISA acceptor beads. When S-RBD binds to ACE2-ECD, the two
81 beads come into close proximity. Upon illumination at 680 nm, the donor beads generate

82 singlet oxygen molecules that diffuse to acceptor beads and transfer energy to thioxene
83 derivatives in the acceptor beads resulting in light emission at 520-620 nm. The results
84 showed that the incubation of ACE2-ECD-Biotin with S-RBD-His produced very strong
85 AlphaScreen signal, and the signal decreased to the basal level in the absence of either of
86 the two proteins (Fig. 1b). To confirm the specificity of this AlphaScreen system, we
87 replaced S-RBD-His with His-tagged extracellular domains of other membrane proteins,
88 including mucosal vascular addressin cell adhesion molecule 1 (MAdCAM-1) and vascular
89 cell adhesion molecule 1 (VCAM-1). Co-incubation of MAdCAM-1-His or VCAM-1-His
90 with ACE2-ECD-Biotin did not generate AlphaScreen signal, indicating that the system
91 detects S-RBD—ACE2 interaction specifically (Fig. 1c).

92 **High-throughput screening of small molecules blocking S-RBD—ACE2 interaction**

93 Next, we used the AlphaScreen-based high-throughput system to screen small molecules
94 that block S-RBD—ACE2 interaction. A total of 3581 small molecule compounds with
95 known molecular structures from FDA Approved Drug Library, Spectrum Collection and
96 Targetmol-Natural Compound Library were assessed (Fig. 1d). The assay was conducted
97 at a final compound concentration of 10 μ M and the interaction between S-RBD-His (0.1
98 μ M) and ACE2-ECD-Biotin (0.2 μ M) was analyzed. After first round screening, 75
99 candidate compounds were identified, which showed inhibitory effect on S-RBD—ACE2
100 interaction (Fig. 1d). All these compounds showed over 45% inhibition rate according to
101 the changes in AlphaScreen signal. To exclude the interference of the compounds to the
102 AlphaScreen system per se, we designed a negative selection system in which the
103 biotinylated S-RBD-His links streptavidin-coated Alpha donor bead and anti-His-
104 conjugated AlphaLISA acceptor bead together to generate AlphaScreen signal directly (Fig.

105 1e). After the negative selection, 10 compounds, including bleomycin sulfate, levodopa,
 106 norepinephrine, trientine hydrochloride, ceftazidime, chiniofon, hematein, theaflavin,
 107 bleomycin and myricetin, from the 75 candidate compounds were validated to inhibit S-
 108 RBD—ACE2 interaction effectively. Among the 10 compounds, ceftazidime was the most
 109 potent inhibitor which showed a relative inhibition rate of 80.7% (Fig. 1f). Thus,
 110 ceftazidime was selected for further investigation considering the best inhibitory effect on
 111 S-RBD—ACE2 interaction, the anti-inflammatory effect and the minimal side effect of
 112 this drug compared with the other 9 compounds¹⁴⁻¹⁷ (Fig. 1g).



113

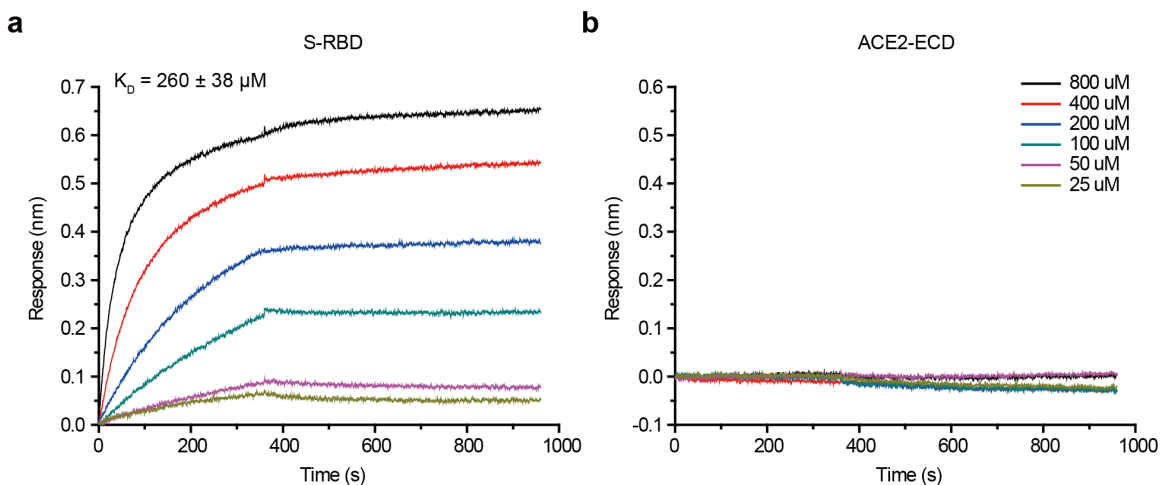
114 **Fig.1 | Screening of small molecule compounds that specifically block the interaction**
 115 **between S-RBD and ACE2.** **a**, Schematic diagram of AlphaScreen system to detect the
 116 interaction between S-RBD and ACE2-ECD. The donor and acceptor beads are coated with
 117 streptavidin and anti-His monoclonal antibody, respectively. **b**, The interaction between S-

118 RBD and ACE2-ECD was monitored using AlphaScreen system. **c**, Comparison of the
119 AlphaScreen signal of S-RBD-His, MAdCAM-1-His and VCAM-1-His proteins in the
120 presence or not of ACE2-ECD-Biotin in AlphaScreen system. **d**, Libraries used in
121 AlphaScreen-based high-throughput system and 75 candidates were identified from 3581
122 compounds in positive selection. The inhibition rate was calculated by the decrease of
123 AlphaScreen signal of each compound compared with that of DMSO vehicle control group.
124 **e**, Schematic diagram of negative selection using AlphaScreen system. Biotinylated S-
125 RBD-His simultaneously links streptavidin-coated donor bead and anti-His-conjugated
126 acceptor bead together to generate AlphaScreen signal directly. **f**, Relative inhibition of 10
127 candidate compounds on S-RBD-ACE2 interaction using AlphaScreen system. The
128 relative inhibition rate was calculated by subtracting the inhibition rate in negative
129 selection from that in positive selection. **g**, Molecular structure of ceftazidime. Data
130 represent the mean \pm SEM ($n \geq 2$) in **b**, **c** and **f**. *** $p < 0.001$, ns: not significant (Student's
131 t test).

132

133 Ceftazidime specifically binds to S-RBD protein

134 To investigate whether S-RBD or ACE2 is the binding target protein of ceftazidime, we
135 applied a bio-layer interferometry experiment to examine the binding affinity between
136 ceftazidime and S-RBD or ACE2-ECD. Along with the elevated concentration of
137 ceftazidime, this compound showed increased binding to S-RBD protein with an K_D value
138 of $260 \pm 38 \mu\text{M}$ (Fig. 2a). Notably, ceftazidime hardly dissociated from S-RBD, indicating
139 a strong and stable interaction between ceftazidime and S-RBD. By contrast, ceftazidime
140 and ACE2-ECD showed no specific binding signal (Fig. 2b). Thus, ceftazidime binds to S-
141 RBD specifically.

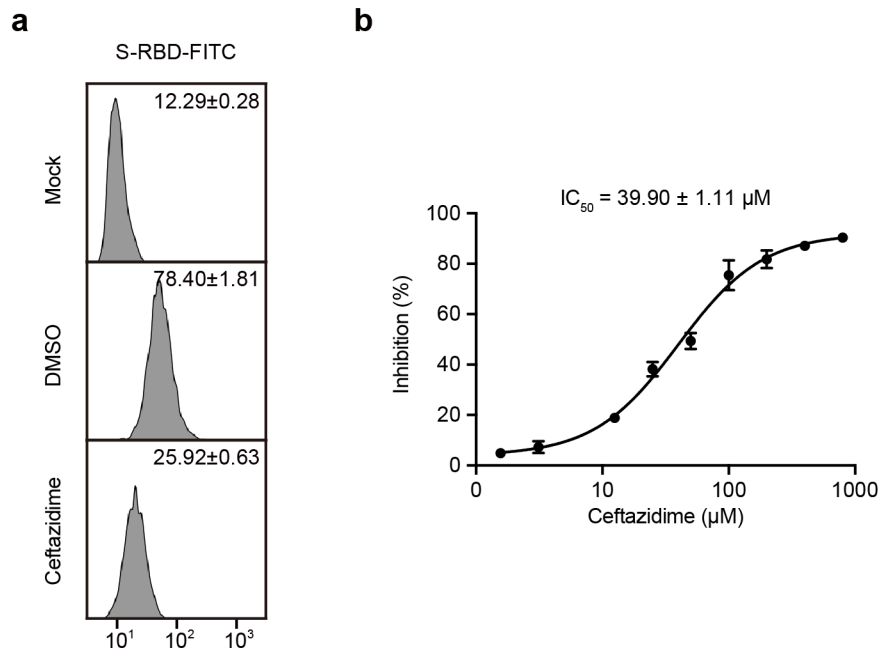


142

143 **Fig.2 | Ceftazidime specifically binds to SARS-CoV-2 S-RBD.** Binding profiles of
144 ceftazidime to S-RBD and ACE2-ECD were measured by bio-layer interferometry in an
145 Octet RED96 instrument. The biotin-conjugated S-RBD or ACE2-ECD was captured by
146 streptavidin that was immobilized on a biosensor and tested for binding with gradient
147 concentrations of ceftazidime.
148

149 **Ceftazidime inhibits S-RBD binding to human pulmonary alveolar epithelial cells**

150 Lung is the main organ infected by SARS-CoV-2, which cause severe acute respiratory
151 syndrome (SARS) ^{18,19}. Therefore, we examined the inhibitory effect of ceftazidime on the
152 binding of S-RBD protein to human pulmonary alveolar epithelial cells (HPAEpiC) which
153 express ACE2. Addition of 100 μ M ceftazidime into the soluble S-RBD binding assay
154 system led to a significantly decrease in the S-RBD binding signal (Fig. 3a), demonstrating
155 the efficient inhibition on S-RBD binding to HPAEpiC cells by ceftazidime. Further
156 analysis showed an IC_{50} of $39.90 \pm 1.11 \mu$ M (Fig. 3b).



157

158 **Fig.3 | Ceftazidime inhibits S-RBD binding to HPAEpiC cells.** **a**, Soluble S-RBD
159 binding to HPAEpiC cells was examined by flow cytometry analysis. Mock, cells were
160 incubated with FITC-conjugated goat anti-human IgG; DMSO, vehicle control;
161 Ceftazidime, 100 μ M ceftazidime in DMSO. Numbers within the panel showed the specific
162 mean fluorescence intensities. **b**, The inhibitory effect of ceftazidime on the binding of S-
163 RBD protein to HPAEpiC cells. Cells were treated with different concentrations of

164 ceftazidime. The inhibition rate was calculated by the decrease of the mean fluorescence
165 intensity of each group compared with that of DMSO vehicle control group. IC₅₀ was
166 indicated in the graph. One representative result of three independent experiments is shown
167 in **a**. Data represent the mean ± SEM (n = 2).

168

169 **Ceftazidime inhibits SARS-CoV-2 pseudovirus infection**

170 Pseudovirus has the similar infectivity compared with authentic virus, thus has been widely

171 applied to carry out the research on the intrusion mechanism of virus with high infectivity

172 and pathogenicity⁴. To evaluate the inhibitory effect of ceftazidime on the entry of SARS-

173 CoV-2 pseudovirus into 293T cells overexpressing human ACE2, we added ceftazidime

174 into the SARS-CoV-2 pseudovirus infection assay system at a series of concentrations. The

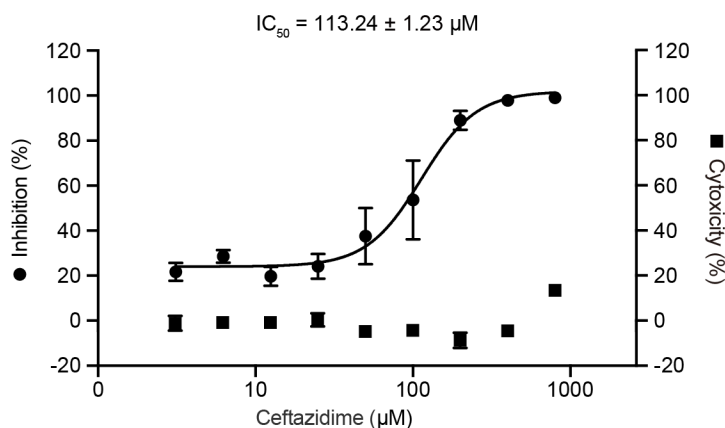
175 results showed that ceftazidime efficiently inhibited SARS-CoV-2 pseudovirus cell entry

176 *in vitro* and the IC₅₀ was 113.24 ± 1.23 μM (Fig. 4). Of note, ceftazidime showed no

177 detectable cytotoxicity at a high concentration of 400 μM, indicating its safety for clinical

178 usage (Fig. 4). Thus, ceftazidime has both anti-bacterial and anti-SARS-CoV-2 effects and

179 should be considered as the first-line antibiotics used for the treatment of COVID-19.



180

181 **Fig.4 | Ceftazidime inhibits SARS-CoV-2 pseudovirus infection.** Inhibition of
182 luciferase-encoding SARS-CoV-2 typed pseudovirus entry into ACE2-expressing 293T
183 cells by ceftazidime. Cells were treated with different concentrations of ceftazidime. IC₅₀
184 was indicated in the graph. The cytotoxicity of ceftazidime to 293T cells was determined
185 by the CCK8 assay. Data represent the mean ± SEM (n ≥ 2).

186

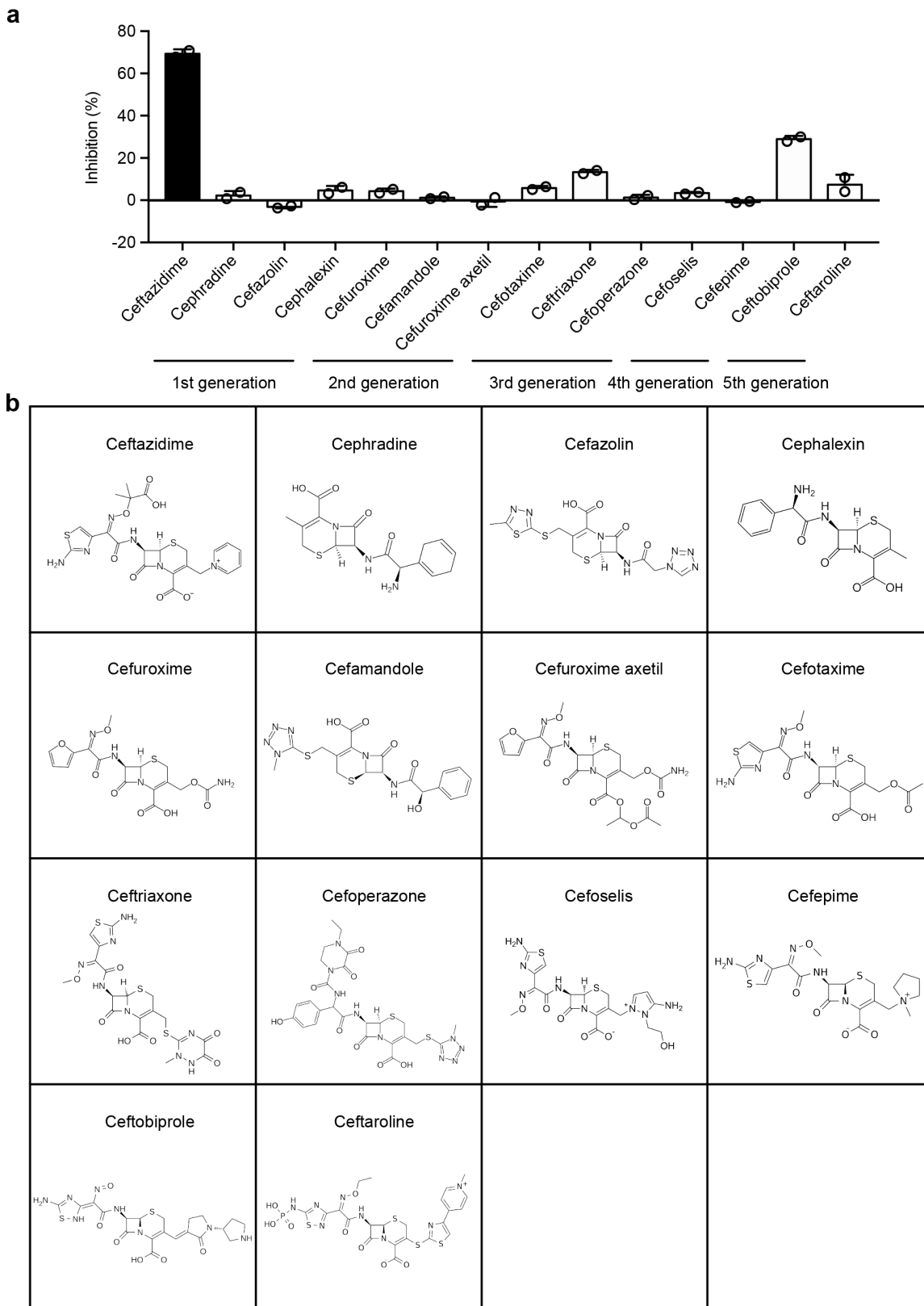
187 **DISCUSSION**

188 Up to date, studies on COVID-19 therapeutics development mostly focus on screening and
189 validation of neutralizing antibodies and the development of vaccine, both require a
190 relatively long time for the effectivity validation and safety assessment. An effective drug
191 with minimal side effect for COVID-19 treatment is eagerly needed. Therefore,
192 repurposing of FDA-approved drugs with minimal known side effects will accelerate the
193 deployment of effective and affordable therapies for COVID-19. In this study, we found
194 that ceftazidime, an antibiotic used for the treatment of pneumonia, has strong inhibitory
195 effect on SARS-CoV-2 pseudovirus cell entry *in vitro* by inhibiting the S-RBD–ACE2
196 interaction. It is noteworthy that ceftazidime has anti-SARS-CoV-2 cell entry and anti-
197 bacterial infection dual functions with little known side effects, which make is ready for
198 immediate preclinical and clinical trials for the COVID-19.

199 Ceftazidime has been widely used in the treatment of bacterial infections. Compared
200 with other compounds that we identified showing inhibition on S-RBD–ACE2 interaction,
201 ceftazidime has less toxicity and side effects. Except for the patients with allergic history
202 of cephalosporins, most COVID-19 patients can be treated with this drug. Ceftazidime has
203 been clinically used as a drug for the treatment of bacterial pneumonia and the blood
204 concentration of ceftazidime can reach over 300 μM . At this concentration, ceftazidime
205 showed an 96% inhibition of SARS-CoV-2 pseudovirus infection *in vitro*, indicating its
206 strong potency to inhibit cell entry of SARS-CoV-2.

207 Cephalosporins have many derivatives which share the similar core structure but have
208 different side-chain modifications. We have also compared the inhibitory effects of 14
209 different cephalosporins, including ceftazidime, cephadrine, cefazolin, cephalexin,

210 cefuroxime, cefamandole, cefuroxime axetil, cefotaxime, ceftriaxone, cefoperazone,
211 cefoselis, cefepime, ceftobiprole and ceftaroline. Among all cephalosporins, only
212 ceftazidime showed strong inhibition on the S-RBD–ACE2 interaction. Ceftobiprole and
213 ceftriaxone showed limited inhibitory effects, whereas other cephalosporins have little or
214 no inhibitory effect on S-RBD–ACE2 binding (Extended Data Fig. 1). These results in
215 combination with a preliminary Structure Activity Relationship (SAR) analysis suggested
216 that the unique moieties in ceftazidime, including 2-aminothiazole, oxime protected with a
217 terminal-exposed isobutyric acid and the positive charged pyridine, might be involved in
218 mediating the binding to S-RBD and eventually blocked the protein interaction between S-
219 RBD and ACE2. Furthermore, our data showed that ceftazidime hardly dissociated from
220 the S-RBD proteins (Fig. 2a), which could be due to the covalent binding of ceftazidime to
221 S-RBD.



222

223 **Extended Data Fig. 1 | Effect of ceftazidime and the derivatives of cephalosporins on**

224 **S-RBD–ACE2 interaction. a**, Inhibition of S-RBD–ACE2 interaction by ceftazidime and
225 the derivatives of cephalosporins was analyzed using AlphaScreen system. **b**, Molecular
226 structures of ceftazidime and the derivatives of cephalosporins. Data represent the mean \pm
227 SEM (n = 2) in **a**.

228

229 In summary, we identify ceftazidime as a potent inhibitor of SARS-CoV-2 pseudovirus
230 cell entry *in vitro* by binding to S-RBD and consequently blocking S-RBD interaction with
231 ACE2. Since ceftazidime is a drug clinically used for the treatment of pneumonia with
232 affordable price and minimal side effects compared with other antiviral drugs, ceftazidime
233 should be considered as the first-line antibiotics used for the treatment of COVID-19,
234 which deserves the immediate preclinical and clinical trials. Optimization of the molecular
235 structure of ceftazidime may further improve the inhibitory effect of this drug on SARS-
236 CoV-2 infection.

237

238

239 **ACKNOWLEDGEMENTS**

240 This work was supported by grants from the National Natural Science Foundation of China
241 (31525016, 31830112), Personalized Medicines-Molecular Signature-based Drug
242 Discovery and Development, the Strategic Priority Research Program of the Chinese
243 Academy of Sciences (XDA12010101), the CAS/SAFEA International Partnership
244 Program for Creative Research Teams, the Youth Innovation Promotion Association of the
245 Chinese Academy of Sciences and the Young Elite Scientist Sponsorship Program by
246 CAST (2019QNRC001). The authors gratefully acknowledge the support of SA-SIBS
247 scholarship program. We thank Prof. Haitao Yang and Dr. Zhenming Jin from
248 ShanghaiTech University for providing the plasmids expressing spike protein and ACE2,
249 and Dr. Xu Han from Shanghai Institute of Materia Medica, Chinese Academy of Sciences
250 for helpful discussion on the structure of the compounds.

251 **AUTHOR CONTRIBUTIONS**

252 C.D.L. and J.F.C. designed experiments. C.D.L., Y.L., M.Y.Y., M.W.H., C.L., H.D., X.C.P.
253 and Y.T.W. performed experiments and analyzed data. X.Y.X. and C.Q.X. provided SARS-
254 CoV-2 pseudoviruses. C.D.L., Y.L. and J.F.C. interpreted results. The manuscript was
255 drafted by C.D.L., Y.L. and edited by J.F.C.

256 **DECLARATION OF INTERESTS**

257 The authors have filed a patent (202010956550.6) for the application of ceftazidime and
258 its derivatives in inhibiting SARS-CoV-2 infection.

259 REFERENCES

- 260 1 Callaway, E., Cyranoski, D., Mallapaty, S., Stoye, E. & Tollefson, J. The
261 coronavirus pandemic in five powerful charts. *Nature* **579**, 482-483,
262 doi:10.1038/d41586-020-00758-2 (2020).
- 263 2 Decaro, N. & Lorusso, A. Novel human coronavirus (SARS-CoV-2): A lesson from
264 animal coronaviruses. *Vet Microbiol* **244**, 108693,
265 doi:10.1016/j.vetmic.2020.108693 (2020).
- 266 3 Ye, Z. W. *et al.* Zoonotic origins of human coronaviruses. *Int J Biol Sci* **16**, 1686-
267 1697, doi:10.7150/ijbs.45472 (2020).
- 268 4 Huang, S. W. *et al.* Assessing the application of a pseudovirus system for emerging
269 SARS-CoV-2 and re-emerging avian influenza virus H5 subtypes in vaccine
270 development. *Biomed J*, doi:10.1016/j.bj.2020.06.003 (2020).
- 271 5 Xia, S. *et al.* Inhibition of SARS-CoV-2 (previously 2019-nCoV) infection by a
272 highly potent pan-coronavirus fusion inhibitor targeting its spike protein that
273 harbors a high capacity to mediate membrane fusion. *Cell Res* **30**, 343-355,
274 doi:10.1038/s41422-020-0305-x (2020).
- 275 6 Wrapp, D. *et al.* Cryo-EM structure of the 2019-nCoV spike in the prefusion
276 conformation. *Science* **367**, 1260-1263, doi:10.1126/science.abb2507 (2020).
- 277 7 Shang, J. *et al.* Cell entry mechanisms of SARS-CoV-2. *Proc Natl Acad Sci U S A*
278 **117**, 11727-11734, doi:10.1073/pnas.2003138117 (2020).
- 279 8 Reguera, J., Ordone, D., Santiago, C., Enjuanes, L. & Casasnovas, J. M. Antigenic
280 modules in the N-terminal S1 region of the transmissible gastroenteritis virus spike
281 protein. *J Gen Virol* **92**, 1117-1126, doi:10.1099/vir.0.027607-0 (2011).
- 282 9 Wang, Q. *et al.* Structural and Functional Basis of SARS-CoV-2 Entry by Using
283 Human ACE2. *Cell* **181**, 894-904 e899, doi:10.1016/j.cell.2020.03.045 (2020).
- 284 10 Chen, X. *et al.* Human monoclonal antibodies block the binding of SARS-CoV-2
285 spike protein to angiotensin converting enzyme 2 receptor. *Cell Mol Immunol* **17**,
286 647-649, doi:10.1038/s41423-020-0426-7 (2020).
- 287 11 Cao, Y. *et al.* Potent Neutralizing Antibodies against SARS-CoV-2 Identified by
288 High-Throughput Single-Cell Sequencing of Convalescent Patients' B Cells. *Cell*
289 **182**, 73-84 e16, doi:10.1016/j.cell.2020.05.025 (2020).
- 290 12 Eroshenko, N. *et al.* Implications of antibody-dependent enhancement of infection
291 for SARS-CoV-2 countermeasures. *Nat Biotechnol* **38**, 789-791,
292 doi:10.1038/s41587-020-0577-1 (2020).
- 293 13 Smatti, M. K., Al Thani, A. A. & Yassine, H. M. Viral-Induced Enhanced Disease
294 Illness. *Front Microbiol* **9**, 2991, doi:10.3389/fmicb.2018.02991 (2018).
- 295 14 Goscinski, G. *et al.* Endotoxin neutralization and anti-inflammatory effects of
296 tobramycin and ceftazidime in porcine endotoxin shock. *Crit Care* **8**, R35-41,
297 doi:10.1186/cc2415 (2004).

- 298 15 Wiedermann, F. J. Anti-inflammatory effects of the antibiotics ceftazidime and
299 tobramycin in porcine endotoxin shock: are they really anti-inflammatory? *Crit*
300 *Care* **8**, 140; author reply 141, doi:10.1186/cc2462 (2004).
- 301 16 Mack, J. M. *et al.* Short-term side effects and patient-reported outcomes of
302 bleomycin sclerotherapy in vascular malformations. *Pediatr Blood Cancer* **65**,
303 e27008, doi:10.1002/pbc.27008 (2018).
- 304 17 Vasta, R. *et al.* Side effects induced by the acute levodopa challenge in Parkinson's
305 Disease and atypical parkinsonisms. *PLoS One* **12**, e0172145,
306 doi:10.1371/journal.pone.0172145 (2017).
- 307 18 Zhang, Y. *et al.* New understanding of the damage of SARS-CoV-2 infection
308 outside the respiratory system. *Biomed Pharmacother* **127**, 110195,
309 doi:10.1016/j.biopha.2020.110195 (2020).
- 310 19 Li, H. *et al.* SARS-CoV-2 and viral sepsis: observations and hypotheses. *Lancet*
311 **395**, 1517-1520, doi:10.1016/S0140-6736(20)30920-X (2020).
- 312 20 Ou, X. *et al.* Characterization of spike glycoprotein of SARS-CoV-2 on virus entry
313 and its immune cross-reactivity with SARS-CoV. *Nat Commun* **11**, 1620,
314 doi:10.1038/s41467-020-15562-9 (2020).
- 315
- 316

317 **METHODS**

318 **Protein expression and purification**

319 Recombinant SARS-CoV-2 S-RBD fused with Fc/His tag (S-RBD-His) was produced in
320 293T cells and purified with Protein A Agarose (Thermo Fisher Scientific). Recombinant
321 human ACE2-ECD fused with Flag/His tag was produced in 293T cells and purified with
322 anti-DYKDDDDK G1 Affinity Resin according to the manufacturer's instructions
323 (GenScript).

324 **AlphaScreen**

325 AlphaScreen assays were performed in Costar 384-well microplates in a 20 μ l final reaction
326 volume. Streptavidin-coated Alpha donor beads or anti-His-conjugated AlphaLISA
327 acceptor beads (PerkinElmer) were used at a final concentration of 10 μ g/mL per well. The
328 assays were performed in PBS buffer (155 mM NaCl, 1.06 mM KH_2PO_4 , 2.97 mM
329 Na_2HPO_4 , pH 7.4) and 0.1% BSA. 5 μ l S-RBD-His (final concentration 0.1 μ M) and 5 μ l
330 ACE2-ECD-Biotin (final concentration 0.2 μ M) were pre-incubated with compounds at a
331 final concentration of 10 μ M for 0.5 h at 4 $^\circ\text{C}$. Then donor beads and acceptor beads were
332 added into the reaction in dark for 2 h, at room temperature. Laser excitation was carried
333 out at 680 nm, and readings were performed at 520 to 620 nm using the EnVision
334 (PerkinElmer) plate reader.

335 **Flow cytometry**

336 0.1 μ M S-RBD-Fc/His was pre-incubated with 5 μ g/mL FITC-conjugated goat anti-human
337 IgG in 50 μ L of PBS and then incubated with HPAEpiC cells for 30 min at room
338 temperature. Cells were washed twice before flow cytometry analysis. Cells were
339 incubated with FITC-conjugated goat anti-human IgG merely as a control.

340 **Pseudovirus infection assay**

341 SARS-CoV-2 pseudoviruses were produced as previously described²⁰. The pseudoviruses
342 were diluted in complete DMEM mixed with an equal volume (50 μ l) of diluted DMSO or
343 ceftazidime, and then incubated at 37 °C for 1 h. The mixture was transferred to 293T
344 expressing human ACE2 stable cell line cells. The cells were incubated at 37 °C for 48 h,
345 followed by lysed with Bio-Lite Luciferase Assay Buffer and tested for luciferase activity
346 (Vazyme). The percent neutralization was calculated by comparing the luciferase value of
347 ceftazidime treatment group to that of DMSO control.

348 **Bio-layer Interferometry (BLI) Experiment**

349 The BLI experiment was performed using an Octet Red 96 instrument (ForteBio, Inc.).
350 Briefly, biotinylated S-RBD or ACE2-ECD (50 μ g/ml) were immobilized on streptavidin
351 (SA) biosensors and then incubated with gradient concentrations of ceftazidime in kinetics
352 buffer (PBS and 0.02% Tween-20). The association and dissociation steps were set to 360
353 s and 600 s. The KD value of the S-RBD binding affinity for ceftazidime was calculated
354 from all the binding curves based on their global fit to a 1:1 Langmuir binding model with
355 an R² value of ≥ 0.95 . Binding experiments were performed at 25 °C. Data were analyzed
356 using Octet Data Analysis Software 9.0 (ForteBio, Menlo park, CA, USA).

357 **QUANTIFICATION AND STATISTICAL ANALYSIS**

358 Statistical significance was determined by Student's t test (GraphPad, version 5.01). The
359 resulting p values are indicated as follows: ns, not significant; *, p < 0.05; **, p < 0.01;
360 ***, p < 0.001. Data represent the mean \pm SEM of at least two independent experiments.

361